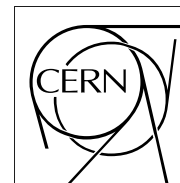**The Compact Muon Solenoid Experiment**

CMS Note

Mailing address: CMS CERN, CH-1211 GENEVA 23, Switzerland

09 June 2006

Measurement of Spin Correlation in Top Quark Pair Production in Semi-Leptonic Final State

M. Baarmand, H. Mermerkaya, I. Vodopiyanov

Florida Institute of Technology, Melbourne, USA

Abstract

The measurement of correlation between spins of top and anti-top quarks, produced in proton-proton collisions at LHC, is described for the semi-leptonic decay of the top quark pair (one top quark decaying leptonically and the other hadronically). The simulated events are reconstructed after full simulation of the CMS detector. The spin correlation coefficient is estimated based on a total integrated luminosity of ten inverse femtobarns. Including systematic uncertainties, the correlation coefficient can be measured with a total relative uncertainty of 17% or 27% depending on the choice of the decay angles used.

1 Introduction

Because of its large width of 1.4 GeV/c^2 the top quark decays before either hadronization, governed by the scale Λ_{QCD}, or depolarization, governed by the scale Λ_{QCD}^2/m_t, can take place. This unique feature is used to investigate the spin of the top quark; such investigation is not possible in the case of light quarks, where the spin information is diluted by hadronization. Moreover, the top quark spin flip time is much larger than its lifetime and the probability of a spin flip due to emission of one or several gluons via chromomagnetic dipole transition is very small. Therefore, the angular distributions of the top quark decay products allow determination of the top quark spin and search for possible deviations from the Standard Model couplings. The present measurement of spin correlation, performed at Tevatron [1], is limited by the small sample of top quarks collected.

At LHC, the top quark is copiously produced in hadroproduction of $t\bar{t}$ pairs. The dominant Standard Model top quark decay mode is $t \to W^+ b$; $W^+ \to l^+ \nu_l$ or $W^+ \to q\bar{q}$ (and charge conjugate mode). The angular distribution of a daughter particle [2, 3, 4] can be written as

$$\frac{1}{\Gamma}\frac{d\Gamma}{d\cos\theta_i} = \frac{1}{2}(1 + \kappa_i \cos\theta_i)\,, \tag{1}$$

where the decay angle θ_i is defined as the angle between the direction of motion of the daughter particle i and the chosen spin axis. The spin analyzer quality κ_i of the top quark daughter particle is defined as the degree to which the daughter particle is correlated with the top spin. Table 1 gives the κ_i values for several top decay daughter particles.

Table 1: Spin analyzer quality κ of the top quark daughter particle.

i	l^+, $\bar{d}$, $\bar{s}$	ν_l, u, c	b	W^+	lower energy q
κ	1	-0.31	-0.41	0.41	0.51

At LHC, the top quarks are mostly produced via gluon fusion (87.5%) and quark-antiquark annihilation (12.5%) [5]. This leads to the helicity basis choice, when the $t\bar{t}$ momentum in the partonic center-of-mass frame is used as the spin axis. The spin correlation in the semileptonic $t\bar{t}$ decay channel (one W decay leptonically and the other hadronically) can be measured in terms of a double differential lepton and quark angular distribution, which (neglecting higher order QCD corrections) is given by

$$\frac{1}{N}\frac{d^2N}{d\cos\theta_l\, d\cos\theta_q} = \frac{1}{4}(1 - \mathcal{A}\kappa_l\kappa_q \cos\theta_l \cos\theta_q)\,. \tag{2}$$

Here, using the helicity basis the lepton and quark angles θ_l and θ_q are obtained by measuring the angle between the decay particle momentum in its parent (anti) top quark rest frame and the (anti) top quark momentum in the $t\bar{t}$ quark pair rest frame. The correlation coefficient

$$\mathcal{A} = \frac{N_\| - N_X}{N_\| + N_X} = \frac{N(t_L\bar{t}_L + t_R\bar{t}_R) - N(t_L\bar{t}_R + t_R\bar{t}_L)}{N(t_L\bar{t}_L + t_R\bar{t}_R) + N(t_L\bar{t}_R + t_R\bar{t}_L)}\,, \tag{3}$$

where $N_\|$ and N_X give the number of events with parallel and anti-parallel top quark spins, respectively. In this paper, distributions of two angle combinations are considered: θ_l versus θ_b and θ_l versus $\theta_{q(\text{lower energy})}$; in the following description these two combinations are denoted as $b - t\, l - t$ and $q - t\, l - t$. The κ values for these daughter particles, b quark and the lower energy (in the top rest frame) quark from W decay, are -0.41 and 0.51, respectively. The latter is estimated as a statistical average for the lower energy jet, since the flavor of the light quark can not be determined in jet measurements.

The estimated cross section for $t\bar{t}$ production at LHC, at the next-to-leading order level, is $830\,\text{pb}$ [6]; for an integrated luminosity of $10\,\text{fb}^{-1}$ this results in $2.46 \cdot 10^6$ events in the semileptonic final state, where in the leptonic branch only electron and muon are considered (branching fraction is 24/81). This represents the "signal" event sample.

The $t\bar{t}$ production, with spin polarization taken into account in the subsequent decay of the top quarks, is simulated with the TOPREX Monte Carlo [7]. The generated double differential angular distributions are presented in Figure 1.
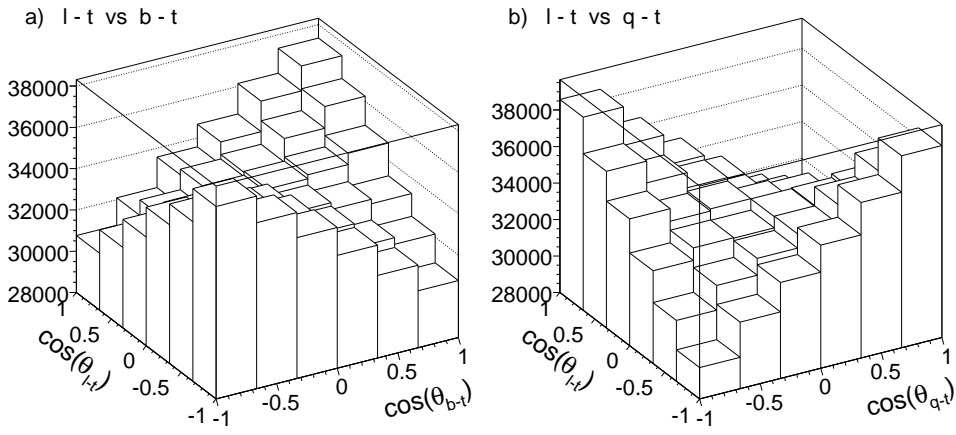
Figure 1: TOPREX generated double differential distribution of the cosine of lepton and quark in the helicity basis: a) l-t angle θ_{l-t} versus b-t angle θ_{b-t}, b) l-t angle θ_{l-t} versus jet$^{\min}$-t angle θ_{q-t}.

The distributions in Figure 1 are fitted, according to Formula (2), with the following function

$$P_1(1 - P_2 \cos\theta_1 \cos\theta_2) \,. \tag{4}$$

Then, from parameter P_2 and using the appropriate κ_i the correlation coefficients are obtained:

$$\mathcal{A}_{b-t\,l-t} = 0.345 \pm 0.007 \,(\text{stat.}) \text{ and}$$
$$\mathcal{A}_{q-t\,l-t} = 0.351 \pm 0.005 \,(\text{stat.}) \,,$$

where the statistical relative errors of 2% are governed by the number of events in the sample ($1.22 \cdot 10^6$). The results are found to be independent, within errors, of the number of $\cos\theta$ bins, varied from 4×4 to 9×9 bins. Note that the value of $\mathcal{A}$ depends of the choice of Parton Distribution Function (PDF); the above results are obtained using the GRV94L PDF (see Section 5).

2   Simulation of Signal and Background Events

Since the available TOPREX Monte Carlo data sample with full detector simulation has insufficient number of events to perform estimations with good precision, a fully detector simulated $t\bar{t}$ event sample ($3.11 \cdot 10^6$ $t\bar{t}$ inclusive decay events) generated with PYTHIA [8] is used. The PYTHIA event generator does not simulate spin correlation between t and $\bar{t}$ in $t\bar{t}$ production. Its double differential angular distributions are flat, see Figure 2. Fitting these distributions, the following correlation coefficients are obtained:

$$\mathcal{A}_{b-t\,l-t} = 0.001 \pm 0.011 \,(\text{stat.}) \text{ and}$$
$$\mathcal{A}_{q-t\,l-t} = -0.001 \pm 0.009 \,(\text{stat.})$$

Therefore, the PYTHIA $t\bar{t}$ events are weighted according to Formula (2) with correlation coefficient $\mathcal{A} = 0.32$ and using appropriate values of κ. Note that $\mathcal{A} = 0.32$ from Reference [7] is chosen for this purpose; the exact input $\mathcal{A}$ value is not important as the analysis aim is to extract the input value with good precision.

Then, this data sample is subdivided into two subsamples: one is regarded as the "reference" subsample (1.61M events), used for the determination of the selection efficiency and background subtraction. The other is regarded as the "analysis" subsample (1.50M events), used for the measurement of $\mathcal{A}$. This subsample provides 436K "signal" events; the remaining 1.07M events with the final states different from the signal are regarded as background and denoted by $t\bar{t}$ "background". The weighted double differential angular distributions obtained from the "analysis" subsample are presented in Figure 3.

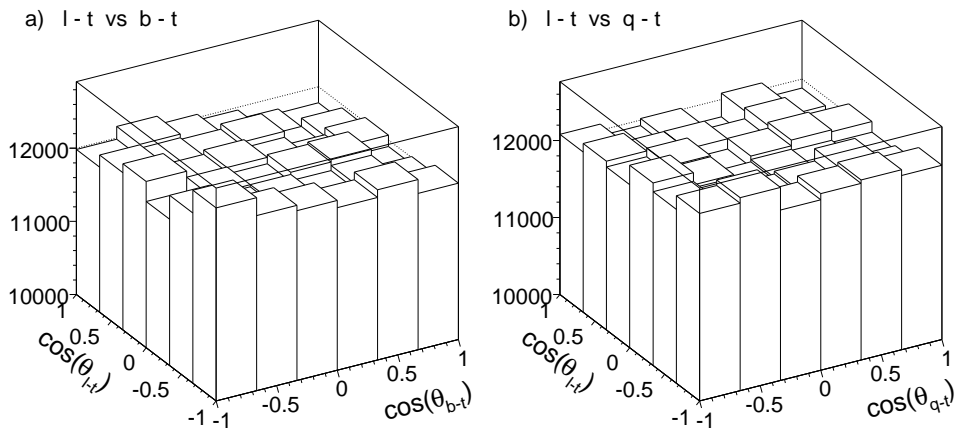Fitting these distributions, the following correlation coefficients are obtained:

3

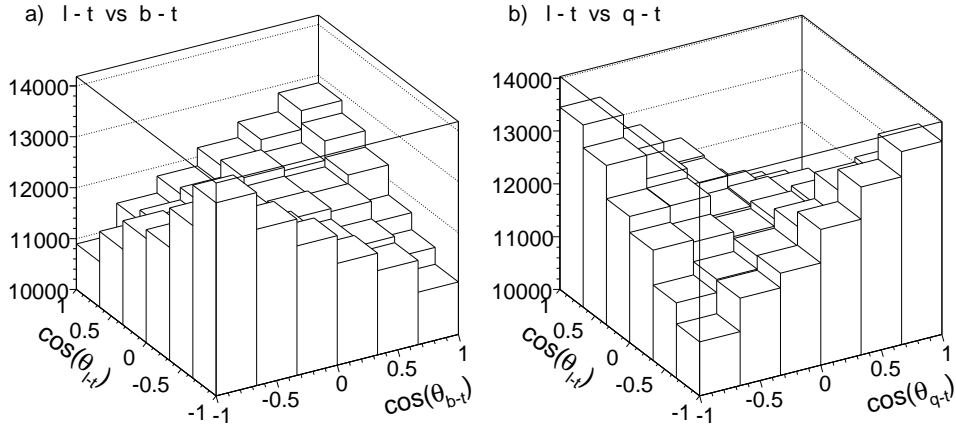Figure 2: PYTHIA generated double differential distributions with no spin correlation.

Figure 3: Double differential distributions obtained from the "analysis" subsample, see text.

$$\mathcal{A}_{b-t\,l-t} = 0.321 \pm 0.011 \text{ (stat.)} \text{ and}$$
$$\mathcal{A}_{q-t\,l-t} = 0.319 \pm 0.009 \text{ (stat.)}$$

The signal and background processes considered are listed in Table 2. The non-$t\bar{t}$ background samples are also generated using PYTHIA and include full CMS detector simulation. The contribution of general QCD events to the background is estimated to be negligible [9].

Table 2: The physics processes considered for signal and background. Efficiencies ϵ are given for different selection steps. The number of selected events for the non-$t\bar{t}$ processes are scaled to the same $t\bar{t}$ sample luminosity.

Process	Simulated events	σ(pb)	ϵ L1+HLT	ϵ topology	ϵ final	Selected events
$t\bar{t}$ (signal)	436K	246	0.55	12.2%	4.95%	21589
$t\bar{t}$ (background)	1.07M	584	0.12	$1.6 \cdot 10^{-2}$	$4.0 \cdot 10^{-3}$	4236
WW + jets	310K	188	0.21	$1.3 \cdot 10^{-3}$	$4.5 \cdot 10^{-5}$	15
W + jets ($\hat{p}_T = 20 - 400$ GeV/c)	2.06M	43K	0.25	$9.1 \cdot 10^{-5}$	$3.4 \cdot 10^{-6}$	260
Wbt semileptonic decay	328K	63.1	0.25	$1.1 \cdot 10^{-2}$	$1.3 \cdot 10^{-3}$	144

4

3   Event Selection

The selection goes through the following steps:

- Selection of events with a leading lepton: muon or electron.
- Selection by topology (type, quality and number of reconstructed objects).
- Reconstruction of two top quarks from their decay products.

3.1   Online Selection

At this step events with muon or electron are selected. The level 1 (L1) triggers used are: single muon or single isolated electron, or combinations of those with a central jet, missing energy, or a tau jet. The L1 trigger efficiency for the $t\bar{t}$ "signal" sample is $\epsilon = 84\%$. The high level triggers (HLT) used are: level 3 muon or level 3 electron. The L1+HLT efficiency for the $t\bar{t}$ "signal" sample is $\epsilon = 54.8\%$.

3.2   Offline Selection

The following objects must be reconstructed in an event:

- Missing transverse energy $\not{E}_{T} > 20$ GeV is required to reconstruct the neutrino from the leptonically decaying W boson, see Figure 4.

- At least one isolated lepton:
  Electron with $|\eta| < 2.5$, $p_T > 27$ GeV/c, hits in the pixel detector, the electromagnetic calorimeter energy over track momentum $E_{ECAL}/P > 0.8$, the hadronic energy over electromagnetic energy $E_{HCAL}/E_{ECAL} < 1$, and isolation from hadronic jets associated with the quarks from the top quark decay by requiring angular separation larger than 0.15 rad.
  Muon with $|\eta| < 2.4$, $p_T > 20$ GeV/c, and isolation from any jet with $p_T > 20$ GeV/c by requiring angular separation larger than 0.15 rad.

- At least four jets with $p_T > 30$ GeV/c and $|\eta| < 2.5$ (jets are reconstructed with the iterative cone algorithm with $\Delta R = 0.5$).

- At least two jets are b-tag jets, the combined b-tag algorithm used [10] provides 66% b-tag efficiency in $t\bar{t}$ events.

- At least two jets have no b-tag.

At this stage the signal selection efficiency is 12.2%.

The reconstruction of two top quarks includes the following requirements:

Two non-b-tag jets with an invariant mass in the range $50 - 135$ GeV/c^2, consistent with the W mass, are found.

A b-tag jet which combined with the above reconstructed W gives an invariant mass in the range $130 - 250$ GeV/c^2, consistent with the top quark mass. Both W and top mass ranges are optimized from Monte Carlo studies using reconstructed jets which are matched to the corresponding generated quarks.

In addition to the top quark reconstructed above, another top quark is required based on the other b-tag jet plus lepton and neutrino combination. The neutrino four-vector is determined using transverse missing energy and the W and top masses. The initial values of the p_T and azimuthal angle ϕ of neutrino are taken from the $\not{E}_{T}$ measurements. The initial value of the longitudinal neutrino momentum Pz is obtained from equation $M(l\nu) = M_W$ (in case of two solutions, that which gives better M_t is chosen). Then, the neutrino components are determined by minimizing

$$\chi^2_{lept} = \left(\frac{M(l\nu) - M_W}{\sigma^{lept}_{M(W)}}\right)^2 + \left(\frac{M(bl\nu) - M_t}{\sigma^{lept}_{M(t)}}\right)^2 + \left(\frac{p_T(\nu) - \not{E}_T}{\sigma_{p_T(\nu)}}\right)^2 + \left(\frac{\phi(\nu) - \phi(\not{E}_T)}{\sigma_{\phi(\nu)}}\right)^2 + \left(\frac{Pz(\nu) - Pz}{\sigma_{Pz(\nu)}}\right)^2,$$
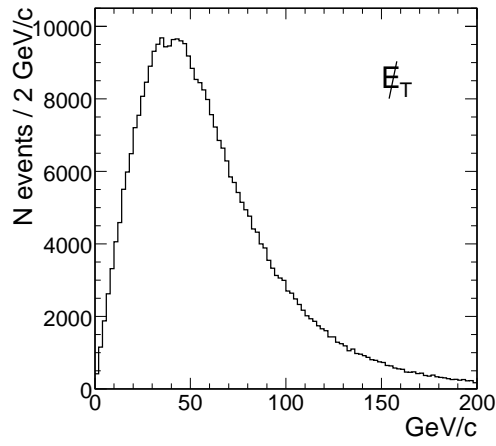
Figure 4: Missing transverse energy distribution in $t\bar{t}$ "signal" sample after trigger selection.

where b represents the b-jet associated with the corresponding b-quark. The resolutions σ are obtained from Monte Carlo using the generated neutrino components and using the other $t\bar{t}$ decay product components reconstructed and matched to the generated ones. The resolutions $\sigma_{\phi(\nu)}$ and $\sigma_{p_T(\nu)}$ are found as the functions of $\not{E}_T$.

Azimuthal angle between the two top quarks is required to be greater than 2 rad.

All the combinations of electron/muon with jets and missing transverse energy, leading to $t\bar{t}$ reconstruction, are tested. The combination with minimal $\chi^2 = \chi^2_{lept} + \chi^2_{hadr}$ is chosen, where

$$\chi^2_{hadr} = \left(\frac{M(q_1 q_2) - M_W}{\sigma^{hadr}_{M(W)}} \right)^2 + \left(\frac{M(b q_1 q_2) - M_t}{\sigma^{hadr}_{M(t)}} \right)^2 .$$

Here b, q_1 and q_2 represent jets associated with the corresponding quarks. The final cut $\chi^2 < 18.5$ (Confidence Level > 1%) is then applied.

This selection results in an overall efficiency of 4.95% (22K events selected out of 436K in the "analysis" subsample). Figure 5 presents the spectra of the reconstructed invariant masses of W and top quarks. The means of the fitted masses are in agreement with the expected values.

A measure of the selection quality (for the $t\bar{t}$ "signal" sample) can be obtained by comparing the generated and reconstructed momentum directions expressed in terms of the cosine of the angles defined above. Figure 6 presents the differences between the generated and reconstructed cosines. Quantifying this selection quality Q as the ratio of the number of events in the four central bins to all bins, one obtains: $Q_{b-t\,l-t} = 52\%$ and $Q_{q-t\,l-t} = 45\%$. The case of $q-t$ angle versus $l-t$ angle looks worse; notice the tail of poorly reconstructed (or mis-selected) lower energy quark jets.

4   Results

4.1   Signal and Background Yields

Figure 7 presents the reconstructed double differential angular distributions obtained from the $t\bar{t}$ "signal" sample. Table 2 summarizes the results of selection for the physics processes considered in this study. The selection efficiencies for different selection steps and the total yields, scaled to the signal luminosity, are shown. In addition to the background contributions tabulated, the contribution from the t-channel single top production is roughly estimated to be 180 events, using the cross section for this process (250 pb) and assuming that its selection efficiency is similar to that of single top production in the associated tW-channel (last row of Table 2).

The $t\bar{t}$ process with decays different from those treated as the signal is the main contribution (87.5%) to the total background. 57% of this $t\bar{t}$ "background" are events with τ lepton(s) in the final state
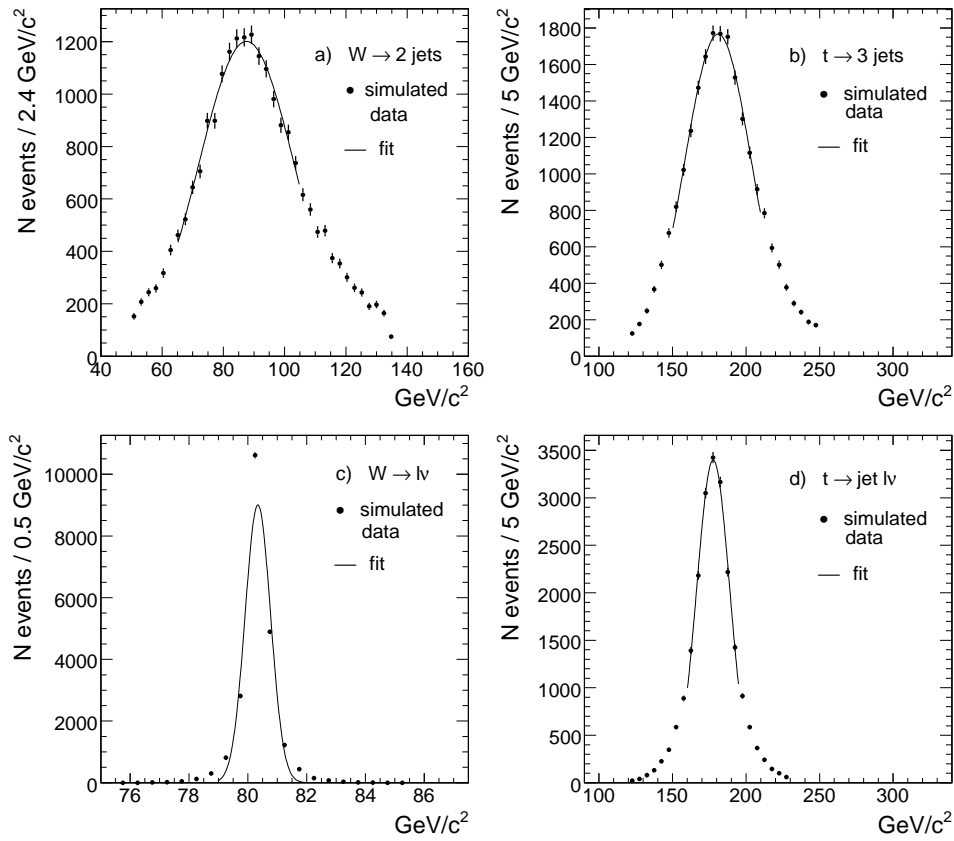
Figure 5: Reconstructed invariant mass spectra: a) W decaying to two jets ($M = 87.6 \pm 0.2\ \mathrm{GeV}/c^2$); b) top quark decaying to three jets, including those from W in (a) ($M = 181.0 \pm 0.3\ \mathrm{GeV}/c^2$); c) W decaying to lepton (e or μ) and neutrino (ν_e or ν_μ) ($M = 80.34 \pm 0.03\ \mathrm{GeV}/c^2$); d) top quark decaying to lepton, neutrino and b-jet (Mean= $177.6 \pm 0.1\ \mathrm{GeV}/c^2$). In c) and d) the widths of W and top are used in the missing energy fit procedure resulting in smaller widths as compared to those in plots (a) and (b).
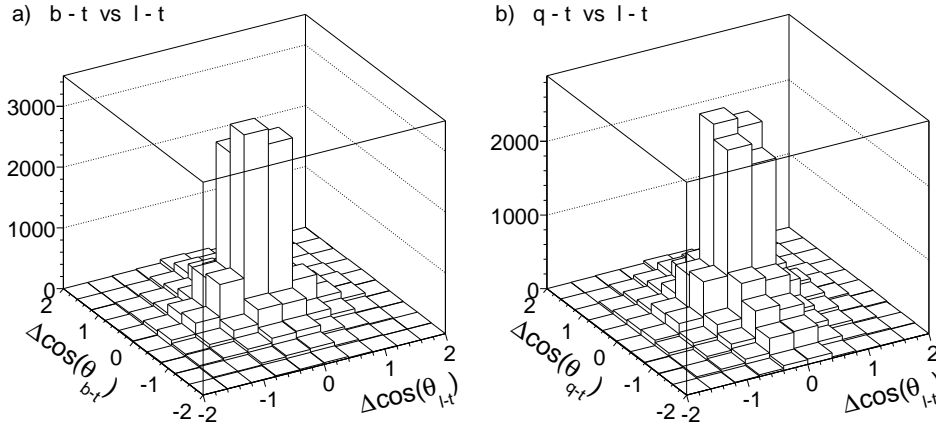

Figure 6: Selection quality: differences between the generated and reconstructed cosines: a) b-t angle versus l-t angle, b) jet$^{\mathrm{min}}$-t angle versus l-t angle.

originating from the $t \rightarrow W \rightarrow \tau \nu_\tau$ decay chain.

Only the $t\bar{t}$ "background" sample, after selection and reconstruction, has significant number of events to be used in the analysis, see Figure 8; the other background samples have very small yields. Therefore, the final all-background sample is obtained from the $t\bar{t}$ "background" scaled to the estimated total number of the background events. The signal to background ratio is found to be 4.5. Figure 9 displays the invariant mass of the reconstructed top quarks plus background and the background only.
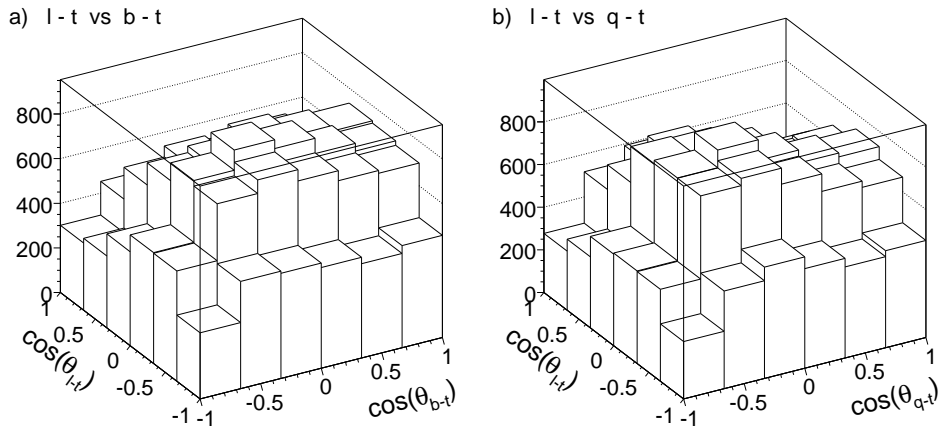
7

Figure 7: Reconstructed double differential angular distribution from $t\bar{t}$ "signal" sample: a) l-t angle θ_{l-t} versus b-t angle θ_{b-t}, b) l-t angle θ_{l-t} versus jet$^{\text{min}}$-t angle θ_{q-t}. No correction for the selection efficiency is applied here.
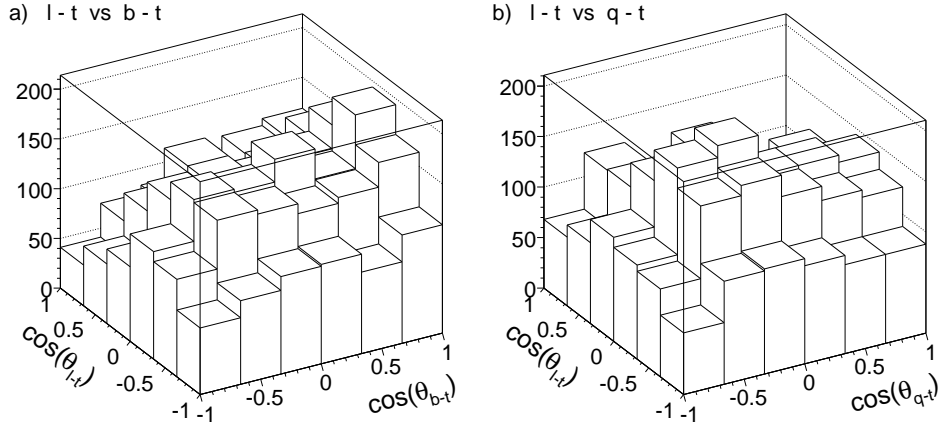

Figure 8: Reconstructed double differential angular distribution from the $t\bar{t}$ "background" sample: a) l-t angle θ_{l-t} versus b-t angle θ_{b-t}, b) l-t angle θ_{l-t} versus jet$^{\text{min}}$-t angle θ_{q-t}.
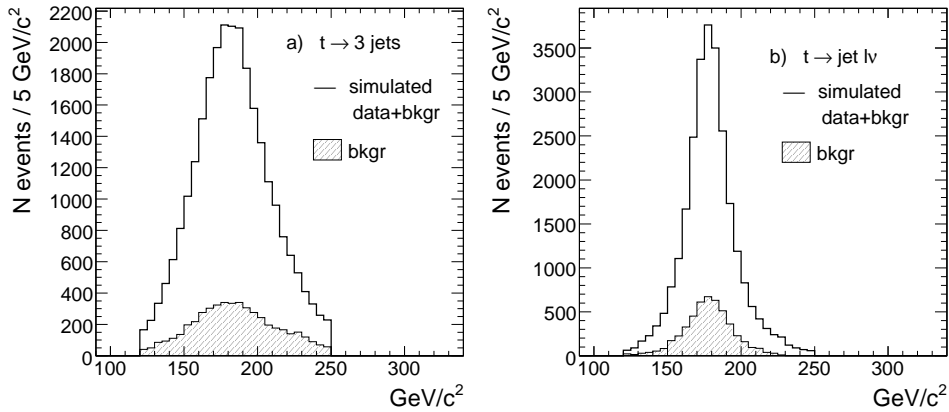

Figure 9: Reconstructed top quark invariant mass spectra: a) top decaying into three jets; b) top decaying into lepton, neutrino and b-jet.

4.2 Differential Selection Efficiency

The double differential angular distributions in Figure 7 are not corrected for selection efficiency. The selection efficiency (6×6) matrix is determined as the ratio of the reconstructed double differential

angular distribution to the generated one, using the the "reference" subsample. The obtained selection efficiency, bin-by-bin, ranges from 2 to 7%, see Figure 10.
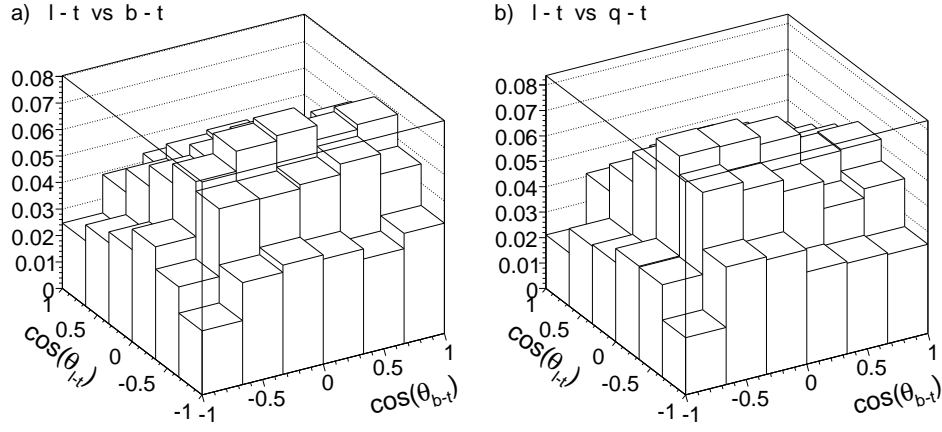

Figure 10: Selection efficiency for double differential distribution of the cosine of lepton and quark: a) l-t angle θ_{l-t} versus b-t angle θ_{b-t}, b) l-t angle θ_{l-t} versus jet$^{\min}$-t angle θ_{q-t}.

4.3   Estimation of the Correlation Coefficient

The final double differential angular distribution is obtained by subtracting, bin-by-bin, the background obtained from the "reference" subsample from the total sample of signal plus background obtained from the "analysis" subsample. The resulting distributions are corrected for the selection efficiency according to Figure 10 and fitted using Formula 4. The final results for the two double differential distributions are shown in Figure 11.
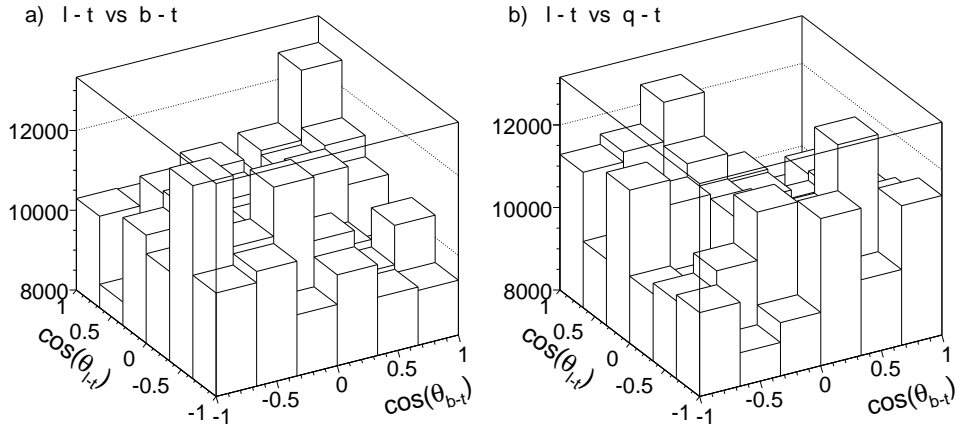

Figure 11: Background subtracted and efficiency corrected double differential distribution of the cosine of lepton and quark in the helicity basis: a) l-t angle θ_{l-t} versus b-t angle θ_{b-t}, b) l-t angle θ_{l-t} versus jet$^{\min}$-t angle θ_{q-t}.

The correlation coefficients obtained from the fit are:

$$\mathcal{A}_{b-t\,l-t} = 0.375 \pm 0.100 \text{ (stat.)} ,$$
$$\mathcal{A}_{q-t\,l-t} = 0.346 \pm 0.079 \text{ (stat.)} .$$

These results agree, within statistical uncertainties, with those obtained from the fits of Figure 3. The expected statistical uncertainty in correlation coefficient for 10 fb^{-1} of integrated luminosity is estimated by the appropriate scaling of the data samples. This gives ± 0.027 for $\mathcal{A}_{b-t\,l-t}$ and ± 0.021 for $\mathcal{A}_{q-t\,l-t}$.

5 Systematic and Theoretical Uncertainties

The following systematic uncertainties are evaluated according to the guidelines in [11]:

PDF's: The choice of the Parton Distribution Function in modeling $t\bar{t}$ production affects the number of $t\bar{t}$ events produced via gluon fusion and that via quark-antiquark annihilation. The relative variation in $\mathcal{A}$, determined using TOPREX with different PDFs (CTEQ6M, MRST2003), is found to be 3.75%.

Top mass: The nominal $m_t = 175 \ \mathrm{GeV}/c^2$ is varied by $\pm 5 \ \mathrm{GeV}/c^2$ [12] using TOPREX. The variation in $\mathcal{A}$ is found to be negligible.

$t\bar{t}$ **cross section:** The uncertainty in the $t\bar{t}$ cross section affects the shape of the final angular distribution after background subtraction; varying $\sigma(t\bar{t})$ by 10% results in 1% relative variation in the correlation coefficients.

b**-tag efficiency:** The selection procedure requires at least two b-tag jets from top quarks decay. Uncertainty due to b-tagging efficiency is evaluated by changing the cut on the b-identification discriminant such that b-tagging efficiency varies from 3.5% to 8% as a function of jet p_T and η [10]. The corresponding relative variation in $\mathcal{A}_{\mathrm{b}-\mathrm{t}\,\mathrm{l}-\mathrm{t}}$ is -20%, and in $\mathcal{A}_{\mathrm{q}-\mathrm{t}\,\mathrm{l}-\mathrm{t}}$ is +6.5%/-8.3%.

JES: The uncertainty due to the jet energy scale uncertainty is evaluated by varying jet p_T from 2.5% to 5% as a function of jet p_T. The relative variation in $\mathcal{A}_{\mathrm{b}-\mathrm{t}\,\mathrm{l}-\mathrm{t}}$ and $\mathcal{A}_{\mathrm{q}-\mathrm{t}\,\mathrm{l}-\mathrm{t}}$ are found to be +7.7%/-14% and -12%, respectively.

Jet multiplicity: Uncertainties in initial and final state radiation, quark fragmentation, underlying events and pile up rate could result in an underestimation of the number of non-$t\bar{t}$ jets (not originating from top decays). The variation in jet multiplicity due to the uncertainties in QCD radiation, quark fragmentation and underlying events is estimated with PYTHIA by counting the number of particles with $p_\mathrm{T} > 5 \ \mathrm{GeV}/c$ generated within $|\eta| < 2.5$ (see section 3.2). The variation in jet multiplicity due to the pile up events (PU) is estimated by comparing two fully reconstructed samples: with PU and without. Table 3 presents the possible contributions of these processes to the jet multiplicity underestimation.

Table 3: Possible background jet multiplicity underestimation due to the uncertainties in simulation of quark fragmentation, underlying events, QCD radiation, and pile up events.

Process	Underestimation (%)
Light quark fragmentation	1.0
Heavy quark fragmentation	1.9
Underlying events	2.2
Initial+final state radiation	6.8
Pile-up events	2.4

This results in a total jet multiplicity underestimation of 7.8%. Production of non-signal jets affects the quality of the selection. To test this effect, 10% additional background jets per event are generated while processing the data sample. Jets are simulated randomly according to the η and P_T distributions of non-$t\bar{t}$ jets, obtained from the $t\bar{t}$ "signal" Monte Carlo. The relative variations in $\mathcal{A}_{\mathrm{b}-\mathrm{t}\,\mathrm{l}-\mathrm{t}}$ and $\mathcal{A}_{\mathrm{q}-\mathrm{t}\,\mathrm{l}-\mathrm{t}}$ are found to be -6.3% and -5.3%, respectively.

6 Conclusion

Summing up in quadrature the systematic uncertainties and using the statistical uncertainties estimated for 10 fb^{-1} of integrated luminosity, the results are:

$$\mathcal{A}_{\mathrm{b}-\mathrm{t}\,\mathrm{l}-\mathrm{t}} = 0.375 \pm 0.027 \ (\mathrm{stat.})^{+0.055}_{-0.096} \ (\mathrm{syst.}) \,,$$
$$\mathcal{A}_{\mathrm{q}-\mathrm{t}\,\mathrm{l}-\mathrm{t}} = 0.346 \pm 0.021 \ (\mathrm{stat.})^{+0.026}_{-0.055} \ (\mathrm{syst.}) \,.$$

In summary, the correlation coefficient of top quark spins in $t\bar{t}$ production is measured with a total relative uncertainty (dominated by systematic uncertainties) of 27% for $\mathcal{A}_{\mathrm{b}-\mathrm{t}\,\mathrm{l}-\mathrm{t}}$ and of 17% for $\mathcal{A}_{\mathrm{q}-\mathrm{t}\,\mathrm{l}-\mathrm{t}}$.

Acknowledgments

References

[1] D0 Collaboration, B. Abbott *et al.*, Phys. Rev. Lett. **85** (2000) 256-261, hep-ph/0002058.

[2] G. Mahlon and S. Parke, Phys. Rev. **D 53** (1996) 4886-4896, hep-ph/9512264.

[3] T. Stelzer and S. Willenbrock, Phys. Lett. **B 374** (1996) 169-172, hep-ph/9512292.

[4] A. Brandenburg, Phys. Lett. **B 387** (1996) 626-632, hep-ph/9606379.

[5] Estimated with the TOPREX [7] Monte Calro sample generated using the GRV94L Parton Distribution Function.

[6] R. Bonciani *et al.*, Nucl. Phys. **B 529** (1998) 424-450, hep-ph/9801375.

[7] S. R. Slabospitsky and L. Sonnenschein, Comput. Phys. Commun. **148** (2002) 87, hep-ph/0201292.

[8] T. Sjöstrand, L. Lonnblad and S. Mrenna, hep-ph/0108264.

[9] J. Heyninck, J. D'Hondt and S. Lowette, CMS NOTE 2006/066.

[10] CMS Collaboration, CERN/LHCC 2006-001, Section 12.2: b-tagging tools.

[11] P. Bartalini, R. Chierici and A. De Roeck, CMS NOTE 2005/013.

[12] K. Hagiwara *et al.*, Phys. Rev. **D 66** (2002).